Solution Conformation, Ion Binding, and Stereochemistry of Griseochelin as Studied by High-field Nuclear Magnetic Resonance Spectroscopy

Lajos Radics* and Maria Kajtár-Peredy
Central Research Institute of Chemistry, P.O. Box 17, H-1525 Budapest, Hungary

The carboxylic acid ionophore antibiotic griseochelin and its Cd^{2+} salt have been studied by ^{13}C (50 MHz), ^{1}H (200 and 400 MHz), and ^{113}Cd (88.73 MHz) n.m.r. spectroscopic methods. Carbon-13 spin–lattice relaxation times, H–D exchange rates of hydroxy protons, and cadmium–proton (metal–ligand) spin–spin couplings have shown that, in non-polar solvents, the essentially open-chain metabolite and its complex salt exist in a conformationally stable pseudocyclic form. This has made it possible to interpret the proton–proton couplings and nuclear Overhauser enhancement data in terms of backbone stereochemistry and to define the relative configurations at all but one of the 13 chiral centres of the molecule, *rel*-(2*S*)-2-{(2*S*,5*S*,6*S*; 9*E*,13*E*)-6-[(1*R*,2*S*,3*S*,4*S*,5*S*,6*R*,11*R*,12*R*)-2,4,6,12-tetrahydroxy-1,3,5,11,13,15-hexamethyloctadeca-9,13-dienyl]-5-methyltetrahydropyran-2-yl}propionic acid or its enantiomer.

Griseochelin (**1**) is a monobasic carboxylic acid ionophore antibiotic isolated recently by Gräfe *et al.*[1,2] from culture filtrates of a modified strain of *Streptomyces griseus*. The metabolite shows biological activity typical of polyether antibiotics, and forms lipid-soluble complexes with divalent inorganic cations (Ca^{2+}, Mg^{2+}, Cd^{2+}, Zn^{2+}, *etc.*) in 2:1 (X_2M) stoicheiometry.[1–3] The elemental composition, $C_{33}H_{60}O_7$, and constitution of the new metabolite were initially inferred from a high-field two-dimensional (2D) proton n.m.r. study.[1] Subsequent chemical and spectroscopic studies[2] have confirmed the n.m.r.-based gross structure; details of the stereochemistry (overall and backbone conformations, sites of ion-binding, and relative configurations at the 13 chiral centres), however, remained undefined. Further n.m.r. experiments were therefore set up and the stereochemical conclusions drawn therefrom constitute the subject of the present paper.

Experimental

Griseochelin was supplied by Dr U. Gräfe (Central Institute of Microbiology and Experimental Therapy, Jena, G.D.R.) and purified as described in ref. 2. The cadmium complex was prepared according to the procedures given earlier.[2] The amorphous material thus obtained was crystallized from $Pr^{i}OH$–MeOH (1:2) to yield colourless needles (m.p. 253—254 °C). The purity of the samples was attested by their n.m.r. spectra.

Bruker AM-400 and WP-200/SY multinuclear instruments were used to obtain the n.m.r. spectra. Carbon-13 spin–lattice relaxation times were measured at 50 MHz and 313 K in 0.2M solutions in $CDCl_3$, using the inversion recovery method. To improve the quality of the relaxation data, composite 90(*X*),180(*Y*),90(*X*) inverting pulse,[4] large data tables, and excessive digital filtering of the free induction decays, collected for 14—16 recovery times, were employed. The transformed data were subjected to three-parameter non-linear least-squares analysis to yield the T_1 values. The overall accuracy of the relaxation data (Table 1) is estimated to be within ±10%. Heteronuclear $^{13}C\{^{1}H\}$ nuclear Overhauser enhancement (n.O.e.) experiments were run to probe the extent of the dipolar mechanism in the ^{13}C relaxation processes. Within experimental errors (10%), the measured n.O.e. values for all proton-bearing carbon atoms were found equal to the theoretical maximum (3.0). The assignments of carbon resonances were inferred from 2D carbon–proton chemical shift correlation experiments run at 50{200} MHz frequency pair.[2]

Table 1. Carbon-13 spin-lattice relaxation times, NT_1/s, of griseochelin and its Cd^{2+} complex[a]

	Free acid	Complex		Free acid	Complex
C-2	0.56	0.21	C-18	0.68	0.45
C-3	0.54	0.21	C-19	0.69	0.46
C-4	0.50	0.28	C-21	0.67	0.52
C-5	0.52	0.28	C-22	1.04	0.65
C-6	0.54	0.25	C-23	1.27	1.12
C-7	0.52	0.26	C-24	2.58	2.46
C-8	0.52	0.21	C-25	7.26	7.20
C-9	0.56	0.27	C-26	3.40	2.70
C-10	0.58	0.27	C-27	3.66	2.40
C-11	0.58	0.27	C-28	3.12	2.10
C-12	0.53	0.22	C-29	3.22	2.45
C-13	0.53	0.27	C-30	3.70	2.05
C-14	0.58	0.35	C-31	3.30	2.40
C-15	0.58	0.40	C-32	3.06	2.14
C-16	0.69	0.40	C-33	3.00	2.02
C-17	0.69	0.40			

[a] 0.2M solution in $CDCl_3$; at 313 K and 50 MHz; assignments based on 2D heteronuclear chemical shift correlation experiments.[2]

Proton–proton coupling constants (Table 2) were derived from 400 MHz conventional (1D) and 2D spectra run at 308 K for dilute solutions (0.01M) in $CDCl_3$ *and* C_6D_6. First, homonuclear 2D chemical shift correlation experiments[5] were performed in order to assign the chemical shifts and coupling pathways of individual protons. Subsequently, *J*-resolved 2D spectra were obtained.[5] The assignment of the individual couplings was assisted by rerunning the 2D *J*-spectra under single-frequency selective decoupling conditions and by comparison with conventional double-resonance proton spectra.

Homonuclear selective $^{1}H\{^{1}H\}$ n.O.e. data were obtained by the difference (d.n.O.e.) method[6] for dilute C_6D_6 solutions of the free acid and its Cd^{2+} salt using the frequency cycling technique[7] for selective preirradiation. Preirradiation times and decoupler power levels were carefully adjusted prior to each d.n.O.e. run and a composite 90(*X*),270(−*X*),360(*X*) (90°)[8] read pulse was employed to eliminate unwanted, frequency-dependent phase distortions along the spectra. Generally, the d.n.O.e. experiments were performed at both 200 and 400 MHz observation frequencies, the former giving larger enhancements, the latter higher selectivities. The free acid and the complex gave qualitatively identical results; therefore only one set of experimental data is reported (Table 3).

Table 2. Proton chemical shifts and coupling constants for griseochelin free acid and its Cd^{2+} complex[a]

	Free acid			Cd complex		
	$\delta_H(CDCl_3)$	$\delta_H(C_6D_6)$	$^nJ_{i,j}$	$\delta_H(CDCl_3)$	$\delta_H(C_6D_6)$	$^nJ_{i,j}$
H-2	3.25	3.35	$^3J_{2,3}$ 11.2; $^3J_{2,33}$ 7.1	3.21	3.49	$^3J_{2,3}$ 11.2; $^3J_{2,33}$ 6.6
H-3	4.03	4.00	$^3J_{3,4A}$ 5.0; $^3J_{3,4B}$ 1.2; $^4J_{3,7}$ 0.4	3.95	4.21	$^3J_{3,4A}$ 5.0; $^3J_{3,4B}$ 1.2; $^4J_{3,33}$ 0.6
H-4_A	1.75	1.45	$^2J_{4A,4B}$ −14; $^3J_{4A,5A}$ 4.0; $^3J_{4A,5B}$ 13.0	1.66	1.57	$^2J_{4A,4B}$ −14; $^3J_{4A,5A}$ 4.0; $^3J_{4A,5B}$ 12.5
H-4_B	1.64	1.31	$^3J_{4B,5A}$ 3.5; $^3J_{4B,5B}$ 3.5	1.59	1.53	$^3J_{4B,5A}$ 3.5; $^3J_{4B,5B}$ 3.5
H-5_A	1.50	1.25	$^2J_{5A,5B}$ −13.6; $^3J_{5A,6}$ 3.5	1.43	1.31	$^2J_{5A,5B}$ −13.5; $^3J_{5A,6}$ 3.5
H-5_B	1.32	1.20	$^3J_{5B,6}$ 10.5	1.34	1.28	$^3J_{5B,6}$ 10.5
H-6	1.62	1.42	$^3J_{6,7}$ 10.2; $^3J_{6,32}$ 6.5	1.52	1.43	$^3J_{6,7}$ 9.7; $^3J_{6,32}$ 6.5
H-7	3.74	3.85	$^3J_{7,8}$ 2.1; $^4J_{7,32}$ 0.4; $^4J_{7,9}$ 0.3	3.81	4.01	$^3J_{7,8}$ 1.2; $^4J_{7,32}$ 0.4
H-8	2.02	1.88	$^3J_{8,9}$ 2.7; $^3J_{8,31}$ 7.1	2.01	1.93	$^3J_{8,9}$ 2.1; $^3J_{8,31}$ 7.1; $^4J_{8,9\text{-OH}}$ 1.2
H-9	3.45	3.40	$^3J_{9,10}$ 10.1; $^4J_{9,11}$ 0.3; $^4J_{9,30}$ 0.4; $^4J_{9,31}$ 0.4	3.33	3.31	$^3J_{9,10}$ 10.1; $^3J_{9,9\text{-OH}}$ 9.0; $^4J_{9,30}$ 0.4
H-10	2.00	2.14	$^3J_{10,11}$ 9.6; $^3J_{10,30}$ 6.7	2.45	2.64	$^3J_{10,11}$ 8.8; $^3J_{10,30}$ 6.8
H-11	3.68	3.64	$^3J_{11,12}$ 2.5; $^4J_{11,13}$ 0.3; $^4J_{11,29}$ 0.4; $^4J_{11,30}$ 0.4	3.68	3.68	$^3J_{11,12}$ 2.6; $^3J_{11,11\text{-OH}}$ 1.0
H-12	1.76	1.53	$^3J_{12,13}$ 2.5; $^3J_{12,29}$ 7.1	1.63	1.48	$^3J_{12,13}$ ~0; $^3J_{12,29}$ 7.1; $^4J_{12,11\text{-OH}}$ 1.8; $^4J_{12,13\text{-OH}}$ 1.2
H-13	4.03	4.15	$^3J_{13,14A}$ 10.2; $^3J_{13,14B}$ 2.2	4.41	4.63	$^3J_{13,14A}$ 10.5; $^3J_{13,14B}$ 2.6; $^3J_{13,13\text{-OH}}$ 1.2
H-14_A	1.75	1.79	$^2J_{14A,14B}$ −13.7; $^3J_{14A,15A}$ 4.6; $^3J_{14A,15B}$ 4.6	1.79	1.74	$^2J_{14A,14B}$ −13.9; $^3J_{14A,15A}$ 4.2; $^3J_{14A,15B}$ 4.2
H-14_B	1.33	1.05	$^3J_{14B,15A}$ 11.3; $^3J_{14B,15B}$ 4.7	1.24	0.97	$^3J_{14B,15A}$ 11.5; $^3J_{14B,15B}$ 4.5; $^4J_{14B,13\text{-OH}}$ 1.0
H-15_A	2.18	2.32	$^2J_{15A,15B}$ −14.2; $^3J_{15A,16}$ 9.4	2.22	2.53	$^2J_{15A,15B}$ −14.2; $^3J_{15A,16}$ 10.5
H-15_B	2.14	2.16	$^3J_{15B,16}$ 3.6; $^4J_{15B,17}$ 1.7	2.13	2.08	$^3J_{15B,16}$ 4.2; $^4J_{15B,17}$ 1.5
H-16	5.49	5.35	$^3J_{16,17}$ 15.2	5.29	5.39	$^3J_{16,17}$ 14.9
H-17	5.35	5.43	$^3J_{17,18}$ 8.9; $^4J_{17,28}$ 0.4	5.55	6.01	$^3J_{17,18}$ 9.7
H-18	2.24	2.31	$^3J_{18,19}$ 9.3; $^3J_{18,28}$ 6.75	2.18	2.44	$^3J_{18,19}$ 9.8; $^3J_{18,28}$ 6.8
H-19	3.58	3.70	$^4J_{19,21}$ 0.5; $^4J_{19,27}$ 0.3; $^4J_{19,28}$ 0.3	3.53	3.86	$^3J_{19,19\text{-OH}}$ 5.3; $^4J_{19,21}$ 0.5; $^4J_{19,28}$ 0.3
H-21	5.11	5.14	$^3J_{21,22}$ 9.5; $^4J_{21,27}$ 1.4; $^4J_{21,26}$ 0.3	4.97	5.17	$^3J_{21,22}$ 9.3; $^4J_{21,27}$ 1.4
H-22	2.42	2.40	$^3J_{22,23A}$ 7; $^3J_{22,23B}$ 7; $^3J_{22,26}$ 6.7	2.40	2.42	$^3J_{22,23A}$; *ca.* 7; $^3J_{22,23B}$ *ca.* 7; $^3J_{22,26}$ 6.7
H-23_A	1.28	1.27		1.27	1.24	
H-23_B	1.20	1.23		1.20	1.20	
H-24	1.24	1.27	$^3J_{24,25}$ 6.9	1.25	1.30	$^3J_{24,25}$ 6.9
H-25	0.87	0.90		0.87	0.89	
H-26	0.93	0.97	$^6J_{26,27} \leqslant 0.2$	0.93	0.97	
H-27	1.59	1.68		1.62	1.78	
H-28	0.85	0.91		0.75	1.05	
H-29	1.12	1.22		1.13	1.43	
H-30	0.67	0.50		0.56	0.42	
H-31	1.08	1.15		1.07	1.17	
H-32	0.78	0.68		0.79	0.77	
H-33	1.14	0.96		1.06	1.33	
9-OH				5.07	5.32	
11-OH				6.95	7.73	
13-OH				6.59	7.17	
19-OH				5.17	5.94	

[a] Chemical shifts (in p.p.m.) relative to internal $SiMe_4$; assignments based on 2D chemical shift correlation experiments (see Experimental section). Coupling values less than 1 Hz were estimated on the basis of the cross peak intensity in COSY experiments. Mutual couplings are given only once, at their first occurrence in the Table.

Single frequency ^{113}Cd and broad-band decoupled $^{113}Cd\{^1H\}$ spectra were obtained at 88.73 and 88.73{400} MHz. Attempts to detect ^{113}Cd—^{13}C couplings proved unsuccessful.

Results and Discussion

Overall Molecular Conformation and Ion Binding.—Polyether antibiotics, the commonest of the naturally occurring carboxylic acid ionophores,[9] owe their ion-transporting properties to the characteristic overall solution conformation, known as a pseudocycle, which favours lipophilic solvent–solute interactions and renders the polar groups inaccessible to nonpolar solvents. Imposed on the ionophore by conformational constraints, intramolecular hydrogen bonds, and solvent—solute interactions, these secondary structures are generally stable, and do not change substantially upon ion binding or releasing.[9,10] Unlike most of the other known polyethers, which contain a number of tetrahydro-furan and/or -pyran systems in their backbones, enhancing the overall conformational stability, griseochelin features a basically open-chain backbone.[11] Yet solubility and related biological properties of the free acid and its salts suggested[1,2] that the metabolite assumes a folded secondary structure in solutions with nonpolar solvents and, in fact, early i.r. spectra have provided support for this contention by indicating the occurrence of intramolecular H-bonding between the distant CO_2H (or CO_2^-) and 19-OH groups in both solid and solution states.[2] Since the success of the stereochemical assignment of the open-chain molecular backbone by n.m.r. methods is intimately linked with the

existence and conformational stability of a well defined secondary structure, additional n.m.r. data were collected to characterize the overall conformation.

As noted earlier,[1,2] owing to the CO_2H-induced mutual exchange of the labile protons, the OH resonances were not detected in the spectrum of the free acid even in highly aprotic solvents and at reduced temperatures. These resonances however do appear as separate multiplets in the spectra of the salts with divalent cations illustrated for the Cd^{2+} complex in the Figure. Addition of D_2O to the $CDCl_3$ solution of this salt at ambient temperature causes the four OH resonances to decrease only slowly in their intensity: the time required to reach one half of the initial signal intensity was approximately 40 min for each OH group. While the uniformity of the exchange rates attests to the occurrence of (slow) mutual proton exchange between the individual alcoholic functions (a fact also verified by a series of selective saturation transfer experiments), the low rate constants indicate that the OH groups are inaccessible to water molecules. Clearly, this situation can only arise if the metabolite occurs predominantly in a folded overall conformation in which each polar group points 'inward' and becomes 'shielded' by the nonpolar outer surface of the molecule.

The polar region thus formed is of primary importance for the ion-transporting properties of the metabolite. Divalent cations. preferentially conveyed by griseochelin,[1-3] have co-ordination number 6. According to carbon-13 chemical shift data,[2] two of the dative bonds are engaged in binding the cation to the carboxylate groups of the two ligands. A direct identification of the remaining sites of ion binding was offered by the ^{113}Cd n.m.r. data of the salt. The broad-band decoupled $^{113}Cd\{H\}$ spectrum displayed a single narrow resonance at -18 p.p.m. [relative to external 0.1M-$Cd(ClO_4)_2$ in water], a value typical of Cd^{2+} ions co-ordinated to oxygen atoms;[12] the observed 1 Hz linewidth provided a lower estimate for the life-time of the

Table 3. Relevant selective n.O.e. data for the Cd^{2+} complex[a]

Irradiated proton(s)	Resonances affected (% n.O.e)
H-2	H-7 (5)
H-7	H-2 (7); H-8 (7); H-10 (6.5); 9-OH (6)
H-9	H-8 (6); H-11 (7); 9-OH (8); H-31 (3)
H-11	H-9 (7.5); 11-OH (9); H-29 (2)
H-13	H-10 (6); 13-OH (7); *H-10 (7); H-12 (5); H-16 (2)*
$H\text{-}14_B$	*H-13 (2.5); H-14$_A$ (10); H-16 (3)*
H-16	H-18 (8)
H-17	$H\text{-}15_A$ (6); H-19 (14)
H-19	H-17 (7); H-21 (14); 19-OH (10); H-28 (3); H-33 (2)
H-21	H-19 (11)
9-OH	11-OH (5)
11-OH	H-10 (3); H-11 (9); 9-OH (8)
13-OH	H-13 (5.5); $H\text{-}15_A$ (4.5)
19-OH	H-2 (9); H-13 (5); H-18 (6)
H-26	*H-21 (4); H-22 (9)*
H-27	H-18 + H-22 (8)
H-28	*H-18 (7.5); H-19 (3); H-21 (2)*
H-29	H-11 (13); 11-OH (2)
H-30	*H-8 (8); H-9 (3); H-10 (4); H-11 (3); H-12 (4); H-13 (4)*
H-31	*H-6 (2.5); H-8 (5); H-9 (6.5); 9-OH (3)*
H-32	*$H\text{-}5_B$ (3); H-6 (5); H-7 (3); H-8 (7)*
H-33	*H-2 (2); H-3 (5); H-19 (2.5)*

[a] In C_6D_6. Italics refer to measurements at 400 MHz. The accuracy of the enhancement data is estimated to be within $\pm 20\%$.

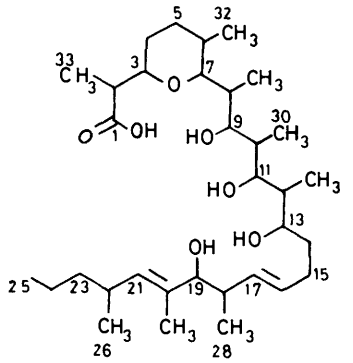

(1)

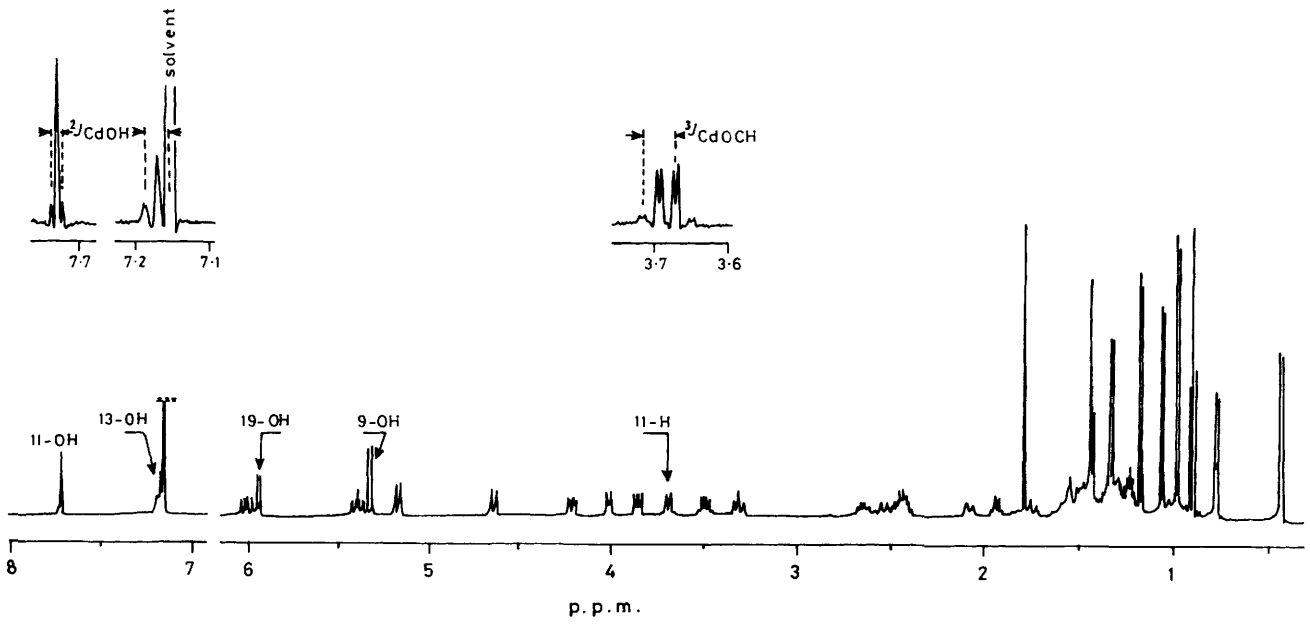

Figure. 400 MHz Proton spectrum of griseochelin cadmium complex in C_6D_6. Expanded, resolution-enhanced multiplets show satellites due to couplings to the cadmium ion

co-ordinated state. In the absence of proton decoupling, the ^{113}Cd resonance appeared as a multiplet, indicating spin–spin couplings to three different protons of the ligands. These were readily identified by closer inspection of the proton spectrum, which displayed low-intensity satellites around the multiplets due to C(11)OH, C(13)OH, and H-11, as shown in the insets to the Figure. [The intensity of the satellites reflects spin–spin coupling of the pertinent protons to both spin 1/2 isotopes of Cd, ^{111}Cd (12.75%) and ^{113}Cd (12.25%).] Although the interpretation of the observed ^{113}Cd—^{1}H couplings, $^{2}J_{Cd,11-OH}$ 6.5, $^{2}J_{Cd,13-OH}$ 13.5, $^{3}J_{Cd,H-11}$ 17 Hz, in terms of bond distances and bond angles is not possible owing to the lack of appropriate reference data, the very appearance of these couplings shows that, besides the carboxylate group, oxygen atoms at C-11 and C-13 are also involved in the co-ordination of the cation. This requires that the overall conformation of the two ligands co-ordinated to the metal ion in a symmetric arrangement is such as to allow the formation of an octahedral structure with Cd–O distances of about 25 nm.[11] Molecular models disclose that this places severe restrictions on the available conformational space for the backbone segment C-1 to C-13, *i.e.* the n.m.r.-based torsion angles around C–C single bonds (see later) represent the most preferred rotational states of the main-chain carbon atoms.

The 'closing' of the pseudocycle (and with it, the 'hiding' of the 19-OH group) clearly requires the presence of a conformational 'turn' encompassing carbon atoms C-14 to C-16. Given the apparent absence of conformational constraints in this part of the backbone, such a folding can only exist by virtue of intramolecular H-bonding of 19-OH as suggested by i.r. observations.[2] Inspection of the chemical shift data reported in Table 2 shows that, in $CDCl_3$ solution, the resonance of 19-OH proton occurs at 5.17 p.p.m., a shift value which in 'normal' cases would suggest weak (if any) H-bonding. Literature data on polyether antibiotics[13] however show that similar, medium, shift values of OH protons can be expected whenever the H-bonding involves polar groups (CO_2^- or O atoms) already engaged in dative bonding with a metal ion. [It may be noted that the other OH groups of the cadmium complex also have their resonances within the narrow shift range 5—7 p.p.m. (see Table 2).] Conclusive evidence for the proposed conformational turn maintained by the $CO_2^- \cdots$ H–O–C(19) bridge is provided by the spatial proximity expressed in the mutual n.O.e. of H-19 and H-33 (see Table 3).

The conformational stability of the folded secondary structure can be conveniently probed by means of carbon-13 spin–lattice relaxation times, T_1. The T_1 values of carbon nuclei, which are relaxed by dipolar interactions with directly bonded protons, are inversely proportional to the effective rotational correlation times, τ_{eff} (a measure of molecular dimensions), for isotropic molecular reorientation. For small biomolecules, the term $(\omega_C + \omega_H)^2\tau^2_{eff} \ll 1$ (in this study $\omega_C = 50$ MHz and $\omega_H = 200$ MHz) and the observed relaxation time T_1 is related to τ_{eff} by the equation[14] $\tau_{eff} = (4.72 \times 10^{-11})/NT_1$ where N is the number of directly bonded protons. In the presence of fast internal motion, τ_{eff} depends on both the overall and internal reorientations: $\tau_{eff}^{-1} = \tau_{overall}^{-1} + \tau_{internal}^{-1}$, where $\tau_{overall}$ and $\tau_{internal}$ are the respective reorientational correlation times. In other words, the onset of fast internal rotation of a given C–H pair results in the lengthening of the pertinent relaxation time.

Inspection of the NT_1 data for the free acid (Table 1) shows that the relaxation times for backbone carbon atoms C-2 to C-15 assume a constant (*ca.* 0.55 s) value, while another, slightly higher, constant NT_1 (*ca.* 0.7 s) is characteristic of the main chain atoms C-16 to C-21. The relaxation times then show a steady increase from C-22 to C-25 in the manner typical of carbon atoms in alkyl chains effectively anchored at one end to a slowly reorienting rigid body.[14] On going to the cadmium complex (see Table 1), we observe a similar distribution of relaxation times except that main chain carbon atoms C-2 to C-22 now relax at higher rates, $(NT_1)_{free\ acid}/(NT_1)_{complex}$ being approximately 2 for C-2 to C-13. In view of the fully dipolar nature of the relaxation processes attested by the $^{13}C\{^1H\}$ heteronuclear n.O.e. results and the equal molarity of the solutes in the two experiments (see Experimental section), this finding indicates that, in accordance with the foregoing conclusions, the backbone atoms in this part of the molecule are held rigidly and thus relax predominantly *via* the overall reorientation of the ionophore; the two-fold increase in the relaxation rates reflects the slowing down of the overall diffusion due to the twofold increase in the molecular dimensions upon complexation. By similar, qualitative, reasoning, the increase in NT_1 values observed at C-16 of the free acid can be interpreted by assuming that, in addition to the overall reorientation, the C–H pairs in the segment C-16 to C-21 also experience the effects of an internal conformational motion which we have tentatively assigned to libration around the C(15)–C(16) bond. Inspection of the pertinent relaxation data for the cadmium complex shows that a slow increase of NT_1 values commences at C-14 and continues up to C-22, to be followed by the more pronounced gradation of the relaxation rates characteristic of freely rotating chain-end alkyl groups. From these observations we may conclude that the H-bond-assisted closing of the pseudocycle leaves in both species some motional freedom available for carbon atoms located outside the rigid C-1 to C-13 zone, the motional freedom being less localized (and apparently more extended) in the complexed form. The limited conformational flexibility of the folded segment presumably provides the ionophore with the means by which it binds the cation and, after having transported it across hydrophobic barriers, releases it. Also, this seems to be responsible for the fact that griseochelin displays only moderate selectivity in binding of divalent cations.[3]

Comparison of the proton–proton coupling constants measured for the ionophore in the uncomplexed and complexed states (see Table 2) shows that both species are characterized by practically the same set of coupling values. This means that, in a similar manner to the cases of polyether ionophores, ion binding (or releasing) does not effect sizeable changes in the preferred backbone conformation of the metabolite. The significance of the minor conformational changes implied in the (small) variations in the coupling values lies presumably in the different lipophilicities (or hydrophilicities) of the two forms as required by the ion-transporting activity of the antibiotic. Following Anteunis,[13] we can estimate the lipophilicity of polyethers by evaluating the sign and magnitude of the aromatic solvent-induced shifts, $ASIS_i = 10^2 \times [\delta_i(C_6H_6) - \delta_i(CDCl_3)]$, for individual protons which, after dissection of protons in the lipophilic [ASIS(−)] and hydrophilic [ASIS(+)] zones, provide the fractional lipophilicity, $f(-)$, and hydrophilicity, $f(+)$, of the molecule with $f(+) + f(-) = 1$ and $f(\pm) = \Sigma ASIS(\pm)/[\Sigma ASIS(+) + \Sigma ASIS(-)]$. By using the chemical shift data for all 55 carbon-bonded protons in Table 2 and performing simple arithmetic, we find that ion binding results in a pronounced decrease in the fractional lipophilicity of the metabolite, $f(-)$ being 0.65 for the free acid and 0.23 for the cadmium salt. The 0.65 value seems to be the highest fractional lipophilicity so far reported for carboxylic acid ionophores, and the nearly threefold decrease in $f(-)$ is believed[13] to be indicative of the fact that the translocation of the cation across the bilayer itself represents the energetically limiting step of the overall transport process.

Backbone Conformation and Stereochemistry.—The existence and conformational stability of the pseudocycle emerging from the foregoing results makes it possible to translate the experimental three- (and, in some instances, four-) bond ^{1}H—

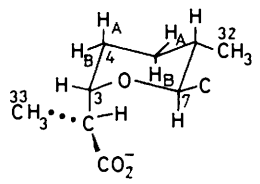

(2)

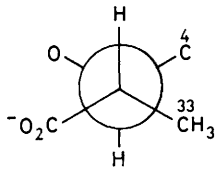

(2a)

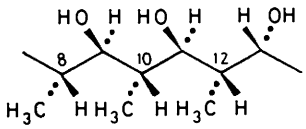

(3)

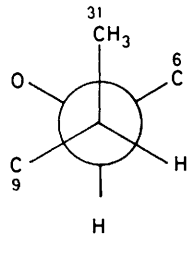

(3a)

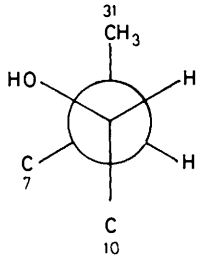

(3b)

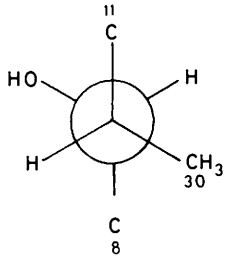

(3c)

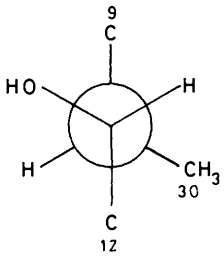

(3d)

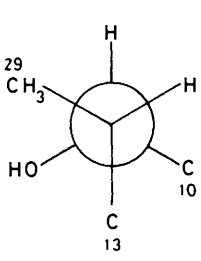

(3e)

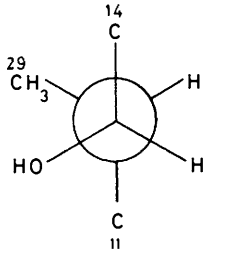

(3f)

^{1}H couplings between backbone protons into torsion angles (φ_i) around formal single bonds and so define the relative stereochemistry at individual carbon atoms. Instrumental in this process are the selective $^1H\{^1H\}$ nuclear Overhauser enhancement data (see Table 3), which provide information on the spatial proximity of various protons and proton groups within the molecule and eliminate thereby eventual ambiguities associated with the use of $J_{HH}(\varphi_i)$ relationships.[7,14] The n.O.e. values, *i.e.* the signal enhancements (in %) originating from through-space dipolar interaction and mutual (cross-) relaxation of protons and observed upon irradiating the resonance due to one of the interacting nuclei, can, in principle, be related to the pertinent internuclear distances.[14] In view of the complexity of the experimental approach, however, no such scope has been pursued in the present study. A brief discussion of the coupling and n.O.e. data will now be given for the example of the Cd^{2+} complex.

Fragment (**2**) (C-1 *to* C-7). The coupling values for protons attached to carbon atoms C-3 to C-7 are typical of substituted tetrahydropyrans in a chair conformation, as frequently encountered with polyether antibiotics,[13] and show that the substituents at C-3, C-6, and C-7 have *axial*, *equatorial*, *equatorial* steric dispositions, respectively. Noting that the substitution causes the chair to assume its $^6C_3$ form (**2**), we can assign the stereochemistries at these chiral centres as α,α,β, or *rel*-3*S*,6*S*,7*S*. Since, furthermore, the carboxylate function must be held in an orientation [around the C(2)–C(3) bond] that points toward the cation, we can settle the relative configuration at C-2 on the basis of the experimental $J_{2,3}$ value (11.3 Hz). Low power selective irradiation of the methyl protons at C-33 causes the H-3 signal to increase in intensity, a finding which requires that the methyl group be aligned synclinal with respect to H-3 or, in other words, that H-3 and H-2 be aligned antiperiplanar [see (**2a**)]. Supporting this conclusion are also the mutual n.O.e. of H-7 and H-2 resonances, by means of which we can define the relative configuration at C-2 as *S*.

Fragment (**3**) (C-8 *to* C-13). While the 2.1 Hz measured for $J_{7,8}$ suggests either synclinal or anticlinal orientation for H-7 and H-8, the n.O.e observed at H-8 and H-6 upon irradiating, respectively, the methyl protons H-32 and H-31, settle this arrangement as synclinal (**3a**) and, with it, define the relative configuration at C-8 as *R*. Arguments outlined in the previous section require that hydroxy functions 9-OH, 11-OH, and 13-OH be oriented 'inward' and the ^{113}Cd–^1H couplings have provided direct evidence that this expectation is fulfilled in the cases of 11-OH and 13-OH. Selective d.n.O.e. measurements at 200 MHz disclosed mutual positive enhancements between hydroxy proton signals of 9-OH and 11-OH, indicating spatial proximity of the two OH groups. (It may be noted that at 400 MHz the positive cross-relaxation effect is outweighed by the negative saturation transfer effect and the difference spectrum displays a negative signal.) This finding, together with the 2.7 Hz measured for $J_{8,9}$, requires that H-8 and H-9 be aligned in a synclinal arrangement, which defines the relative configuration at C-9 as *S* [see (**3b**)]. Selective saturation of the H-30 resonance gives rise to positive difference signals at the H-8 and H-9 resonances. The spatial proximities implied in this result indicate that the value of 10.1 Hz obtained for $J_{9,10}$ reflects an antiperiplanar steric relationship between H-9 and H-10 [see (**3c**)], which defines the relative stereochemistry at C-10 as *S*. With the 11-OH group held oriented toward the cation, the value of 8.8 Hz found for $J_{10,11}$ is again indicative of an antiperiplanar arrangement of H-10 and H-11 [see (**3d**)], and this settles the relative configuration at C-11 as *S*. The assignment of the relative stereochemistry at C-12 and C-13 can be arrived at by similar reasoning. Here we note the enhancements of the H-12 and H-13 signals on saturating the H-30 methyl resonance and that of H-11 when irradiating the methyl doublet due to H-29. Then, by recalling the ion–ligand interaction observed for 13-OH, we find that the $\leqslant$ 2.5 Hz values obtained for both $J_{11,12}$ and $J_{12,13}$ reflect synclinal arrangements for the pertinent protons [see (**3e**) and (**3f**)]. Supporting the steric disposition proposed for H-12 is also the sizeable planar W coupling of this proton to 13-OH. On the basis of these pieces of information the relative configurations at C-12 and C-13 can be assigned as *S* and *R*, respectively.

Fragment (**4**) (C-14 *to* C-25). From the coupling data obtained for the five-spin system H-13,H-14$_A$H-14$_B$,H-15$_A$H-15$_B$ and the occurrence of a planar four-bond coupling between 13-OH and H-14$_B$ we can define the preferred spatial arrangement of protons in the two adjacent methylene groups as depicted in (**4a**) and (**4b**). The resulting spatial proximity of the C-13 and C-16 methine groups associated with the conformational turn is further supported by the enhancement of the H-16 signal upon irradiating at the frequency of the H-13 resonance. The analysis of the coupling patterns of protons H-15$_A$H-15$_B$,H-16 and the occurrence of a 1.5 Hz homoallylic interaction between H-15$_B$ and H-17 have led to assignment of the steric disposition portrayed in (**4c**). Further down the aliphatic chain we note the positive enhancements of H-21,

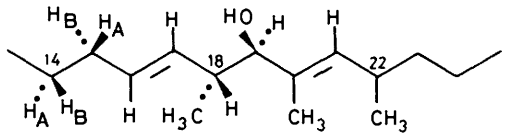

(4)

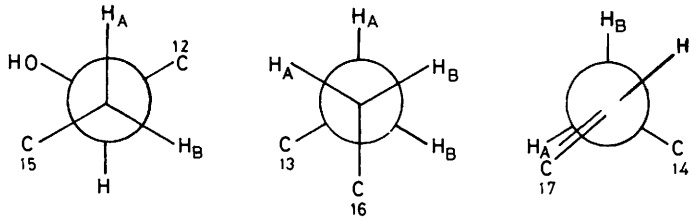

(4a) (4b) (4c)

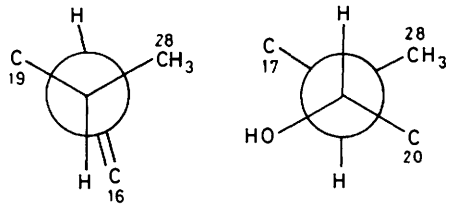

(4d) (4e)

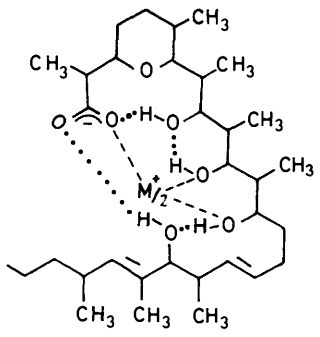

(5)

H-28, and H-33 resonances observable when irradiating the frequency of the allylic proton H-19. This information, combined with measured vicinal couplings of the pertinent protons, allow us to represent the relative stereochemistries at C-18 and C-19 as shown in (**4d**) and (**4c**), respectively, and to assign both these chiral centres the relative *R* configuration. Saturation of resonances due to H-27 and H-19 results in respective enhancements of the H-18 and H-21 signals which, together with the 0.5 Hz (*cis*-allylic) coupling between H-19 and H-21, indicates that H-21 and the methyl H-27 are *trans*-oriented at the 20,21-double bond. The increasing conformational flexibility revealed by the relaxation data for carbon atoms C-22 to C-25 has received confirmation from the observation of motionally averaged vicinal couplings between the pertinent protons. Specifically, the 7 Hz found for both $J_{22,23A}$ and $J_{22,23B}$ precludes any conclusion as to the preferred torsion angles around the C(22)–C(23) bond, which renders the assignment of the relative configuration at C-22, the remaining chiral centre, impracticable.

Hydrogen bonding. The finding that the alcoholic OH groups of the complex display well defined three- and four-bond spin–spin couplings with their adjacent protons indicates the existence of highly preferred local conformations stabilized by intramolecular H-bonds. The available coupling data allowed us to make a tentative mapping of the H-bonding network, shown schematically in (**5**). The 9 Hz observed for $^3J_{9,9\text{-OH}}$ indicates antiperiplanar disposition of the two protons which, according to molecular models, suggests H-bonding interaction with one of the carboxylate oxygen atoms. The mutual n.O.e. between 9-OH and 11-OH together with the near-zero $^3J_{11,11(OH)}$ and the planar W $^4J_{11(OH),12}$ couplings show that H-11 and 11-OH are orthogonal to each other, with H-11 pointing toward the C-9 oxygen atom, a finding that might be indicative of a C(9)O · · · H–OC(11) H-bond. From the coupling data for 13-OH we can conclude that this hydroxy proton is again orthogonal to its CH partner, and points towards C(19)O, to enable C(19)O · · · H–OC(13) interaction. The hydrogen bonding network is then completed with the bridge connecting 19-OH and the CO_2^- group (see before).

Relationship with Zincophorin.—After the completion of this study we learned about the paper by Brooks *et al.*,[15] reporting the *X*-ray-based structure and absolute stereochemistry of zincophorin, a carboxylic acid ionophore possessing the same constitution as griseochelin. In view of the common biological origin (*S. griseus*) and similarities in spectral data, Brooks and his co-workers suggested that the two metabolites may prove to be stereoisomers or possibly even identical. This expectation seems to be reinforced by the results obtained in the present work: the relative stereochemistry at the twelve assigned chiral centres of griseochelin is identical with that reported for zincophorin.

Acknowledgements

We thank Dr. U. Gräfe for supplies of griseochelin. We also thank Dr. L. Szilágyi (Institute of Organic Chemistry,

University of Debrecen, Debrecen, Hungary) and Professor P. L. Indovina (Istituto Superiore di Sanità, Rome, Italy) for permission to use their n.m.r. facilities. Thanks are also due to Dr. M. Incze (Central Research Institute of Chemistry) for the preparation of the Cd complex and purification of the samples.

References

1 L. Radics, *J. Chem. Soc., Chem. Commun.*, 1984, 599.
2 U. Gräfe, W. Schade, M. Roth, L. Radics, M. Incze, and K. Ujszászy, *J. Antibiot.*, 1984, **37**, 836.
3 U. Gräfe, G. Reinhardt, and N. Misoga, *Studia Biophysica*, 1984, **102**, 165.
4 M. H. Levitt and R. Freeman, *J. Magn. Reson.*, 1979, **33**, 473.
5 A. Bax, 'Two Dimensional Nuclear Magnetic Resonance in Liquids,' Delft University Press, 1982.
6 J. K. M. Sanders and J. D. Mersh, *Progr. Nucl. Magn. Reson. Spectrosc.*, 1983, **15**, 353.
7 M. Kinns and J. K. M. Sanders, *J. Magn. Reson.*, 1984, **56**, 618.
8 Ch. Bauer and R. Freeman, *J. Magn. Reson.*, 1985, **61**, 376.
9 J. W. Westley, *Adv. Appl. Microbiol.*, 1977, **22**, 177.
10 Y. Ovchinnikov, V. T. Ivanov, and A. M. Shkrob, 'Membrane Active Complexones,' Elsevier, New York, 1974.
11 B. K. Toeplitz, A. I. Cohen, P. T. Funke, W. L. Parker, and J. Z. Gougoutas, *J. Am. Chem. Soc.*, 1979, **100**, 3344.
12 P. D. Ellis, 'The Multinuclear Approach to NMR Spectroscopy,' eds. J. B. Lambert and F. G. Riddell, Reidel, Dordrecht and Boston, 1983, pp. 457—523.
13 M. J. O. Anteunis, 'Polyether Antibiotics,' ed. J. W. Westley, M. Dekker, New York and Basel, 1983, vol. 2, pp. 245—334.
14 See *e.g.* R. J. Abraham and P. Loftus, 'Proton and Carbon-13 NMR Spectroscopy,' Heyden, London, 1978.
15 H. Brooks, D. Gardner, and J. P. Poyser, *J. Antibiot.*, 1984, **37**, 1501.

Received 5th December 1985; *Paper* 5/2139